Zeitschrift für Geomorphologie, Vol. 61/4 (2018), 315–326
Published online March 2018; published in print June 2018

Article

Spatial and temporal variation of the aeolian sediment transport in the ephemeral Baringak Lake (Sistan Plain, Iran) using field measurements and geostatistical analyses

H.R. Abbasi[1,2]*, C. Opp[1], M. Groll[1], H. Rohipour[2], M. Khosroshahi[2], F. Khaksarian[2], A. Gohardoust[2]

[1] Faculty of Geography, Marburg University, Germany
[2] Desert Division, Research Institute of Forests and Rangelands, Agricultural Research Education and Extension Organization (AREEO), Tehran, Iran
* Corresponding author: abbasi.hamidreza@ymail.com

With 7 figures and 5 tables

Abstract: Wind erosion is one of the most serious problems in the Sistan region, located in the East of Iran and near the border of Afghanistan. During the dry and hot seasons, strong winds locally called the “Sadobist Roozeh”, which means “120 windy days” blow from Northern and Northwestern directions to the Southeast. This wind entrains and transports dust and sand from the dry beds of ephemeral lakes, affecting the Sistan region in Iran, southern Afghanistan and northern Pakistan. In order to investigate the land surface sensitivity to aeolian transport, 74 graduated pins were embedded randomly in the ephemeral Baringak Lake bed and the aeolian transport rates were measured for three events in 2013 individually as well as for the total study period. The spatial and temporal variation of the aeolian transport was also mapped using GIS and geostatistical methods for these events and for the total duration of 103 days. The resulting variograms revealed a high spatial dependence of the different events and showed that geostatistical techniques are a valid tool for the mapping of aeolian sediment transport. The average transport rate in terms of the detected drift height on the dry lake bed was 1.93 cm or 31 kg/m^2 between the 5th of August and the 17th of November in 2013.

Keywords: Wind erosion; geostatistics; Sistan; Iran

1 Introduction

Wind erosion is one of the main land degradation processes, affecting more than one third of the global land surface (Oldeman 1992, Opp 1998, Weinan & Fryrear 1996) and also about 19.7 million hectares in Iran (Ahmadi 1998). The sources of dust and sand storms are usually extensive and the land rehabilitation is extremely costly and time consuming. Thus, the identification of areas with a high sensitivity to wind erosion into the dust and sand sources and their properties is a valuable tool for the selection of prioritized degradation areas for land management measures (Herrmann et al. 1999). The land cover vulnerabilities and wind erosion rates have been studied with different methods on different spatial and temporal scales (Belnap & Gillette 1998, Chepil 1945, Lancaster & Baas 1998, Li et al. 2005, Ravi et al. 2010, Reich et al. 1999, Wolfe & Nickling 1993). While Groll et al. (2013) and Opp et al. (2016) have analyzed the spatial and temporal differentiation of aeolian deposition with the help of deposition samplers around the Aral Kum in Central Asia. Hudson (1993) provided a review of the field measurement of soil erosion and runoff and explained the advantages and disadvantages of these methods as an instrument for getting a first approximation of the amount of erosion in a given situation. One of these reconnaissance methods is the widely used point or pin method (Casagli et al. 1999, Hadley & Lusby 1967, Haigh 1977, Hooke 1980, Takei et al. 1981, Wolman 1959), which is a very simple and cost effective method, requiring hardly any maintenance or staff training. Thus it allows for an extensive and long-term

DOI: 10.1127/zfg/2018/0451
www.borntraeger-cramer.de
0372-8854/zfg/2018/0451 $ 3.00

spatial measurement of aeolian transport processes. In recent years the method has been refined, eg. in the form of photo-electronic erosion pins (Bertrand 2010, Horn & Lane 2006, Lawler 2001, McDermott & Sherman 2009). Combining the spatial array of erosion pins with probability theory based on geostatistical methods of interpolation (Burrough 1986, Hengl 2009, Oliver et al 1989, Robinson & Metternicht 2006, Shi et al. 2003) allows the creation of reliable and detailed water and wind erosion rate maps, which can be important decision support tools for the land use management. Several studies have successfully used geostatistical approaches for mapping the spatial and temporal variation of the sediment transport rate (Chappell et al. 2003a, 2003b, Poortinga et al. 2015, Sterk & Stein 1997, Visser et al. 2004, Uzun et al. 2017), while so far there is no an indication of the application of such as combined approach in Iran.

The Sistan plain is located in the Eastern of Iran, near the border to Afghanistan. It is an alluvial plain in the lower reaches of the Hirmand River and is dominated by a group of six ephemeral lakes called "Hamoun Lakes" and characterized by a very strong wind during the hot season. This wind, locally called "Sadobist Roozeh" or "120 windy days" is formed by a Siberian air stream flowing from Northern and Northwestern direction from the Hindu-Kush mountain range into the Sistan plain lowland between mid-May and mid-September (Alizadeh-Choobari et al. 2014). The water level of the six Hamoun Lakes varies largely and in times of prolonged droughts the lakes desiccate and dry up. When a strong wind blows during the hot and dry season it can easily mobilize the sediments of the dry lake beds, turning the Hamoun Lakes into important sources of dust and sand storms in the Southwest Asia (Goudie & Middleton 2006, Middleton 1986). A particular long drought began in 1999 and the number of dusty days has rapidly increased since that year (Miri et al. 2010), negatively affecting not only the Sistan region but also Southern Afghanistan and Northern Pakistan.

In this study, the collected data of the aeolian sediment transport rate for the Sistan Baringak Lake have been analyzed using a geostatistics approach in order to understand the temporal and spatial dust variation during a four months period in 2013. The main objective of the study was to identify areas sensitive to the aeolian transport as a scientific base for the selection of prioritized areas for erosion mitigation measures.

2 Research Area

The Hamoun lakes are located in the Zabol county of the Sistan and Baluchistan Province (30.2° N–31.5° N; 61.0° E–62.2° E; the average elevation of the lakes and surrounding areas is around 425 m a. s. l.) in Southeastern part of Iran, the second largest of the 31 provinces in the country (Busche et al. 1990). Sistan plain borders to the Nimruz and Farah Provinces in Western Afghanistan and is close to the Chagai district in the Baluchistan Province in Western Pakistan. The total area of the Zabol, Nimruz, Farah and Chagai administrative units is 150,000 km^2, inhabited by approximately one million people.

According to TAVO, the study area is characterized by Quaternary surface and subsurface deposits with Arenosols, Solonchaks, Fluvisols, and salt flats and mud flats of the kavires as well (Busche et al. 1990). The lakes correspond with discontinuous groundwater aquifers with essentially high salinity. The annual precipitation in this region is 100 mm or less (Denk & Müller 1990), 105 mm just near the Afghan border, and 56 mm in the lower Iranian parts of the plain. The annual mean air temperature is relatively high with 21.6 °C. The summers are hot and dry with average temperatures of up to 35 °C and the winters are mild (8 °C) with an average monthly precipitation of 20 mm. This classifies the Sistan plain as a hot desert climate (BWh) after Köppen-Geiger (Peel et al. 2007).

The central element of the Sistan plain is a complex of six lakes (Fig. 1), which are in Persian called Hamoun Lakes, describing their ephemeral character. The Lakes of Hirmand, Chonge Sork, Baringak and some part of the Sabari and Puzak Lakes are located in Iran while the other parts of the Sabari and Puzak Lakes as well as the Gowd-e-Zareh Lake are located in Afghanistan (Table 1). The total area of the lakes is 7,763.6 km^2, 41.5% of which is located in Iran and 58.5% in Afghanistan (Vekerdy et al. 2006). The lake system is supplied by the Hirmand (or Helmand) River, which originates in the Kabul mountains in Afghanistan and flows into Iran. Crossing the borderline between Afghanistan and Iran several river beds of a past inland delta, which fallen dry, can be identified. Its water is mainly used for irrigation farming in the Afghan part of the catchment. During the last 20 years, six dams have been constructed in the upper reaches, mainly for the irrigation water management, and as a result less water reaches the Hamoun Lakes. In combination with a severe drought, starting in 1999, the aeolian dust transport in the Sistan region has significantly increased in recent years (Rashki et al. 2013, Sharifikia 2013, Vekerdy et al. 2006). The very low density of herbaceous and semi-woody salt swamps and the large areas totally without any vegetation accelerate deflation processes in the windiest area of Iran.

The field measurement area selected for this study is the Hamoun-e-Baringak (31.2° N; 61.35° E), which is located between the Sabari and Puzak Lakes near the Iran-Afghanistan border. It is a shallow lake with an area of 221.6 km^2 (Table 1). Water from the Hamoun-e-Puzak

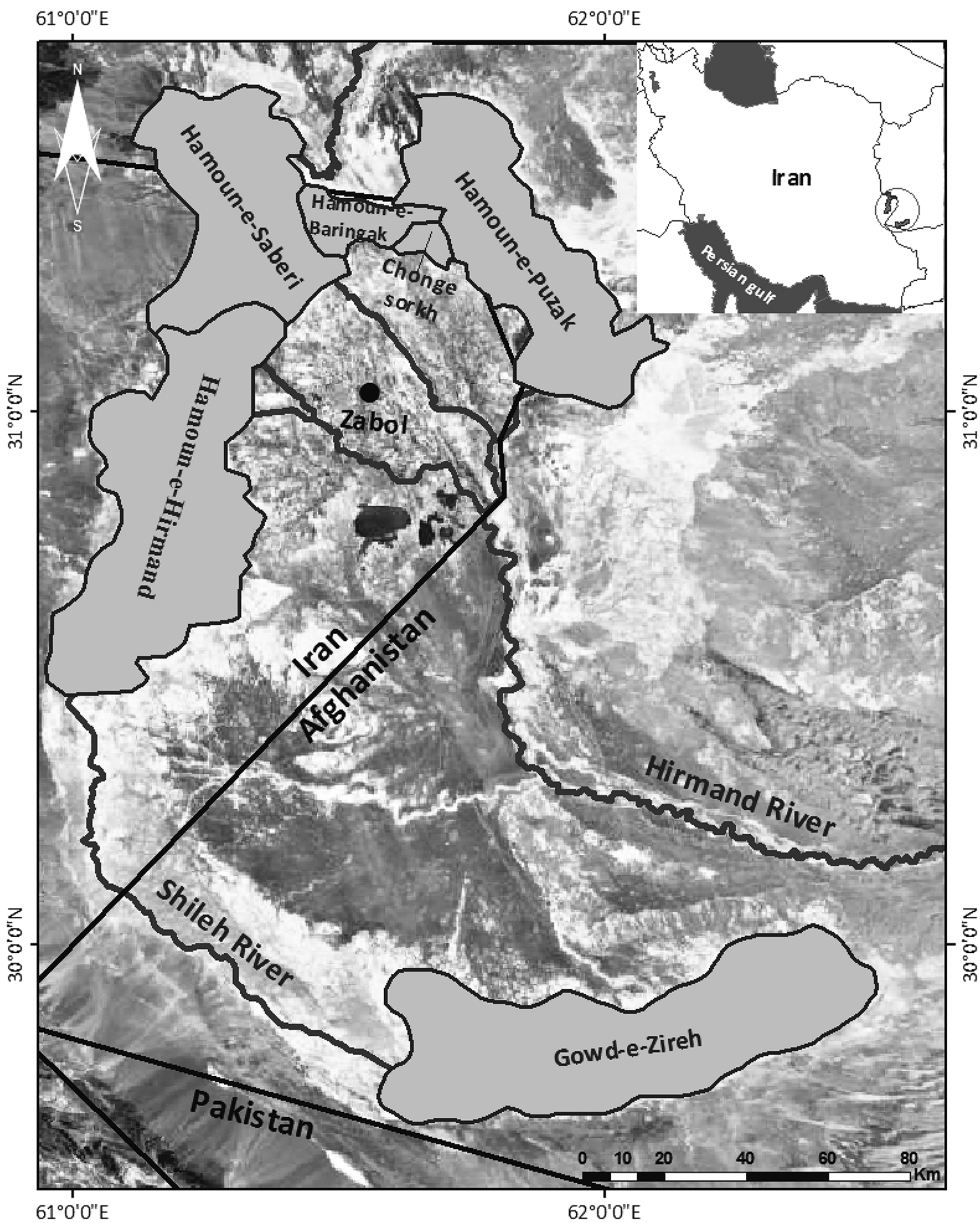

Fig. 1. Location of the Hamouns (ephemeral lakes) in the Sistan plain.

Table 1. Area, average depth and location of the six Sistan Plain lakes (UNEP 2006).

Sistan Plain Hamouns	Average depth (m)	Area (km^2)	Area in Iran (%)	Area in Afghanistan (%)
Baringak	1	221.6	100	–
Chonge Sorkh	1	59.8	100	–
Hamoun Hirmand	2	2,388.8	100	–
Hamoun-e-Puzak	2–3	1,514.4	5.2	94.8
Hamoun-e-Saberi	3	1,161.5	41	59
Gowd-e-Zareh	10	2,417.5	–	100

flows into the Hamoun Saberi via the Baringak Lake during heavy flood events. The Hamoun-e-Baringak is a playa filled with quaternary lacustrine silts and clays, covered by Holocene fluvial sands, silts and clays (Whitney 2006). The west part of lake forms from lacustrine sediments and fluvial sediments in east area. The dominant soils are Entisols or Aridisols (Aqusalids and Torriorthents). The soil texture (based on 48 soil samples) is composed of 24% sand, 43% silt and 33% clay. The topsoil bulk density is 1.6 gr/cm^3, the average electric conductivity is 62 ds/m, and the average pH is 9.

3 Material and methods

For this study a combination of meteorological data, field measurements and geostatistical methods have been used to find spatial and temporal variation of the aeolian sediment transport in the ephemeral Baringak Lake. For the meteorological information, data from the Zabol station were adopted. This station is located 25 km south of the Baringak study area (31°02′ N, 61°50′ E, Fig. 1) at an elevation of 480 m. Wind speed and wind direction data recorded at 10 m above ground level were provided in three-hour intervals for the period from 1994 to 2013 by the IRIMO (I.R. Iran Meteorological Organization). Based on this high temporal resolution data, seasonal wind roses were created in 36 sectors using the frequency of different wind speeds as a percentage of the total winds (Fig. 4). In addition to this long-term analysis, the maximum daily wind speed data for the year 2013 was also plotted against the time (Fig. 5).

In order to monitor the aeolian sand and dust transport, a network of 74 graduated pins were embedded in the soil of Baringak study area (Fig. 2). This study area (20 × 7 km) had been selected based on the interpretation of dust and sand storm satellite images (MODIS 2004) and on-site experiences, showing that the land could be a major sand and dust source in the region. The positions of the pins were determined randomly and then recorded with GPS (Fig. 3). All pins were embedded on the 5th of August 2013 and the aeolian transport rates were measured on the 28th of August, the 15th of September and the 17th of November in 2013.

The collected field data have been used for the generation of variograms in order to analyze the spatial and temporal dependencies of the aeolian transport rate. A variogram is a function describing the degree of spatial dependence of a random spatial random data field or within a stochastic process, and it is a useful tool for the interpretation of the causes of spatial variation (Webster & Oliver 2001). The variogram indicates the degree of similarity among the values of a variable when the samples are separated by sequential distance increments called lag distances, and what this distance is also spatially orientated (Akhavan 2010). The variogram analysis was carried out in GS+ (version 10) for each event of sediment transport using a fitted model based on an ordinary kriging method. The mass transport rates were mapped using the geostatistical analysis extension in ArcGIS (version 9.3).

The mean absolute error (MAE), relative mean absolute error (RMAE), root-mean-square error (RMSE) were used in a second step to assess cross validated models. The best fitted model was selected for the three events as well as for the whole duration, followed by an evaluation of the spatial variations of the aeolian transport rate. Ordinary kriging was used for the spatial interpolation and the results have been cross-validated in order to evaluate the variogram performance.

4 Results and discussion

4.1 Wind data analysis and wind erosion events

The seasonal wind roses (Fig. 4) revealed prevailing winds blowing from northern and north-western directions throughout the year. The wind speed was characterized by strong day-to-day fluctuations of up to 20 m/s (Fig. 5). On average the highest speed winds were registered in spring and summer (6.75 m/s and 9.53 m/s) and were related to the “120 windy days”. During autumn and winter, on the other hand, the average wind velocities were much smaller (3.96 m/s and 3.81 m/s). The long-term (1995–2013) average wind speed was 11.96 m/s and the recorded maximum had been detected on June 13th in 2004 with 29 m/s.

Overall, the wind speed in the Sistan region is relatively high with 69 days (1,687 hours; 19% of all days) exceeding 10 m/s in 2013. Within the study period from the 5th of August to the 17th of November in 2013, this wind speed had been exceeded on 40 days (38% of the days).

The wind characteristics for the three measurement periods are given in Table 2. The highest wind speeds (up to 20 m/s, with an average of 10.3 m/s for all hours with a wind speed ≥7 m/s) were detected during the first period (05.08.2013–28.08.2013), which is still part of the “120 windy days”. This first period was also characterized by the highest percentage of hours with an average wind speed of ≥7 m/s (61.3%). Over the course of the study period the maximum wind speed dropped considerably from 20 m/s to 15–17 m/s and the percentage of hours with a wind speed of ≥7 m/s steadily decreased from 61.3% to 48.6% during the second period and to

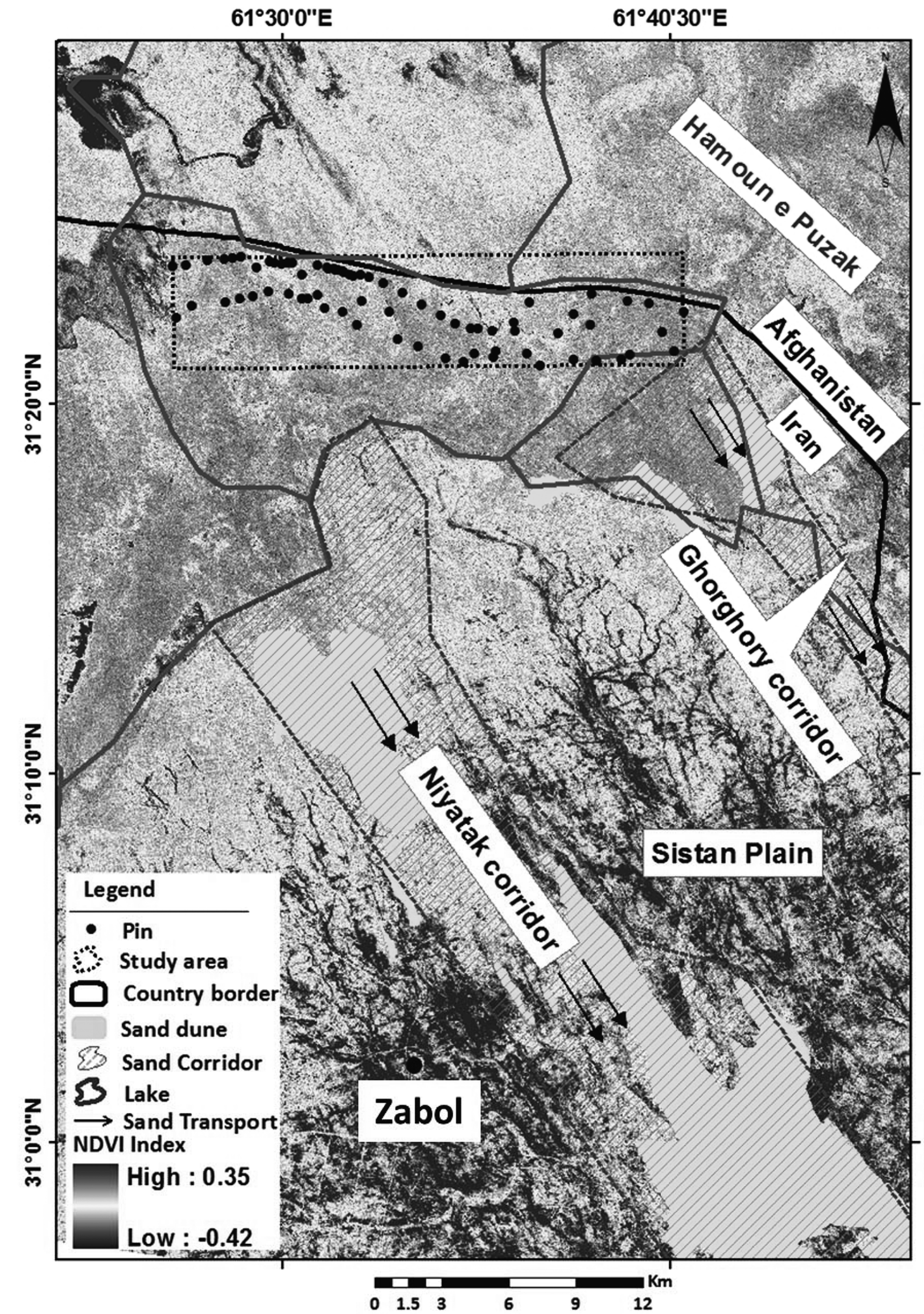

Fig. 2. NDVI for the Sistan Region derived from Landsat-8 ETM + images for the year 2013 and the locations of the installed erosion pins in the Hamoun-e-Baringak and study area, hachure parts show sand corridors.

Fig. 3. Graduated erosion pin (left) and indicators of the wind energy in the Baringak lake (right).

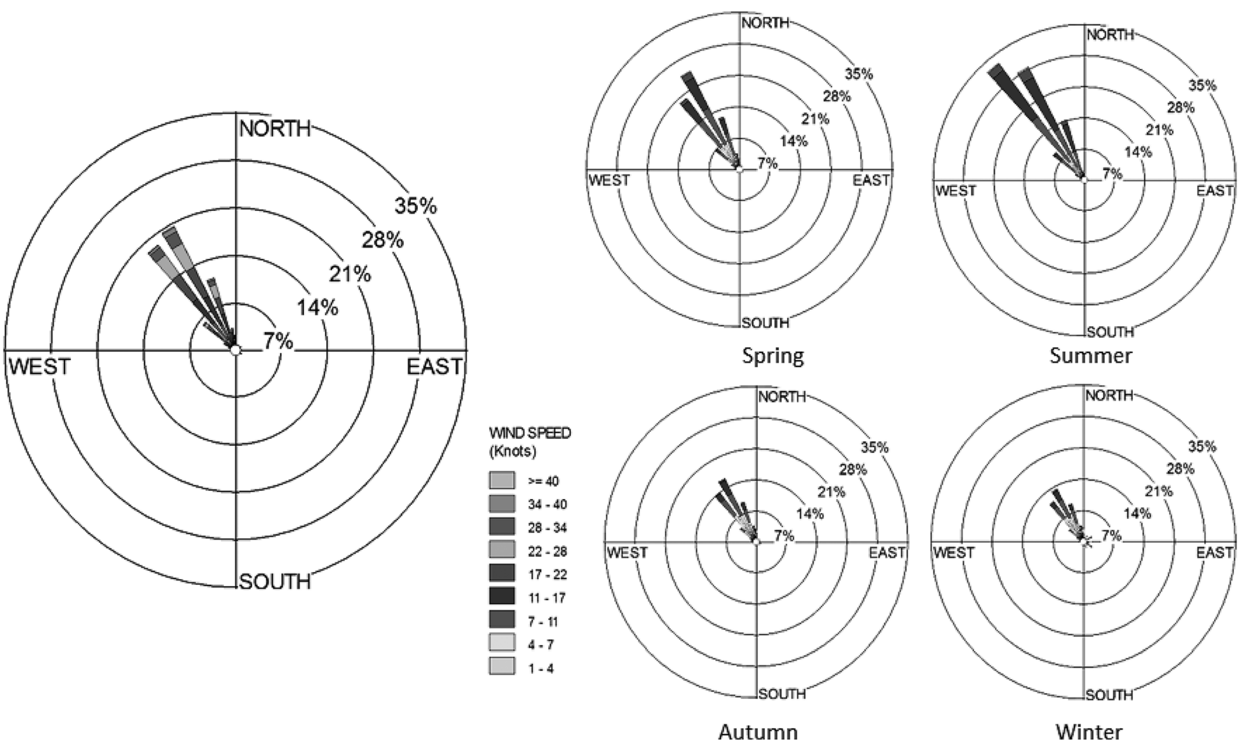

Fig. 4. Annual and seasonal wind roses for the Zabol Meteorological Station for 1995–2013; 36 sectors, with the frequency of different wind speeds as a percentage of the total winds.

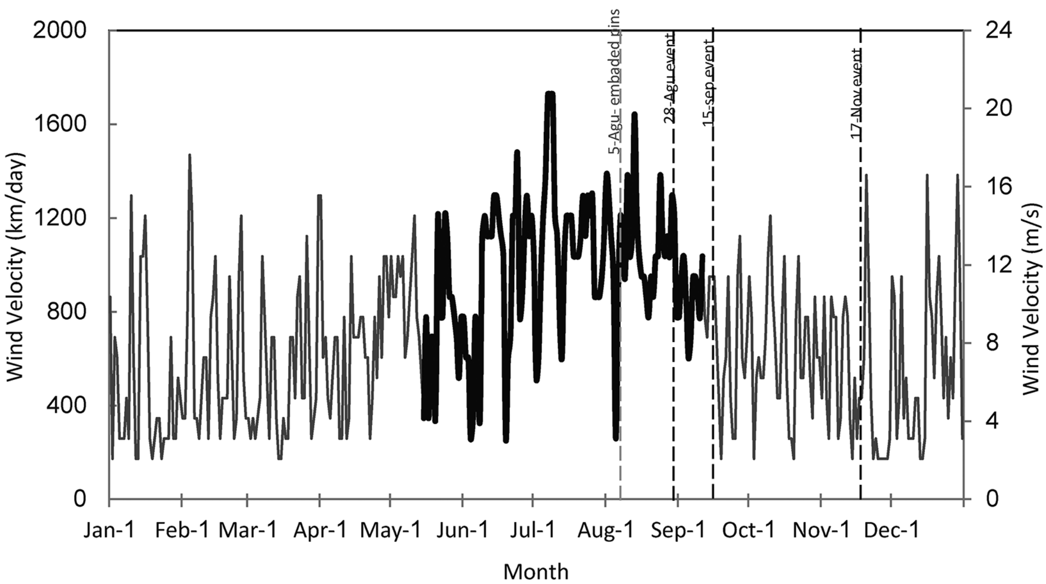

Fig. 5. Maximum daily wind speed at the Zabol meteorological station in 2013. The thicker black line section shows the duration of the "120 windy days"; the black vertical line marks the embedding of the pins and the dashed vertical lines indicate the dates of the transport rate measurements.

Table 2. General characteristics of wind erosion events between August and October 2013 in the Sistan region, based on data from the Zabol meteorological station.

No.	Event and Date	Maximum wind speed (m/s)	Average wind speed of all hours ≥7 m/s (m/s)	Wind duration ≥7 m/s (hours and % of the duration)	Dominant wind direction
1	05.08.2013–28.08.2013	20	10.3	353 (61.3%)	NNW
2	29.08.2013–15.09.2013	15	9.6	210 (48.6%)	NNW
3	16.09.2013–17.11.2013	17	9.3	383 (25.3%)	NNW
4	Total duration	20	9.7	946 (37.5%)	NNW

25.3% during the third period. This emphasizes the meteorological magnitude of the "120 windy days" and its potential for dust and sand mobilization. Throughout the whole period the dominant wind came from NNW, therefore the wind regime can be considered unimodal for this study, which increases the accuracy of the pin measurements.

4.2 Aeolian sediment transport

The meteorological data showed that the Sadobist roozeh wind (120 wind days) period during the summer months has a much higher potential for the dust and sand mobilization and long-distance transport than the autumn and winter seasons. This is also confirmed by the sediment erosion data gathered with the erosion pins. Several sediment transport metrics are provided in Table 3. During the first period (August 2013) both the variability and the mean erosion rate (0–64 kg/m^2 and 17.94 kg/m^2 on average) recorded in the Baringak study area have been much higher than during the following two periods.

The average erosion measured by the pins was 1.12 cm during the first period (Table 3) which equals an erosion rate of 0.53 mm/d. During the second and third period the recorded erosion rates were much lower (0.32 and 0.03 mm/d respectively). During the total duration of 103 days, 1.93 cm of soil was eroded from the Baringak lake bed (30.86 kg/m^2). Based on this erosion rate it can be estimated that 6.84 million tons of lake bed sediments have been eroded from the 221.2 km^2 large Baringak Lake between August and November of 2013.

4.3 Geostatistical analysis

In order to give the point data collected with the erosion pins a spatial dimension, a geostatistical analysis of the

Table 3. Summary statistics of the average transport rates in the Baringak study area.

Dates and events	No. of pins	Min-Max Range (kg/m²)	Mean Transport kg/m²	Mean Transport cm	Median (kg/m²)	Standard Deviation (kg/m²)	Coefficient of Variation (%)	Kurtosis	Skewness
05.08.–25.08.2013	74	0–64	17.94	1.12	16	1.74	102	0.04	0.94
26.08.–15.09.2013	74	0–32	10.64	0.67	8	1.5	98	–0.57	0.75
16.09.–17.11.2013	66	0–16	2.54	0.16	0	0.99	153	2.58	1.7
Total	74	0–80	30.86	1.93	32	1.48	71	–0.65	0.36

Table 4. Results of the cross variogram analysis and the fitted models for sediment transport for the three periods in 2013 at the Baringak Lake.

Period	Model	MSE	Range	Spatially dependent variance C	Nugget Variance C_O	Sill ($C+C_O$)	$C/(C+C_O)$
1.: 05.08.–25.08.2013	Spherical	1.33	1,698	7.17	0.16	7.33	0.97
2.: 26.08.–15.09.2013	Gaussian	1.26	1,579	3.29	0.91	4.83	0.81
3.: 16.09.–17.11.2013	Spherical	0.48	3,569	3.01	0.00	3.01	0.99
Total	Spherical	0.67	4,830	395.30	94.00	489.30	0.81

erosion rate data was conducted. To reduce the skewness of the sample distribution, the data from the first two periods were transformed to square-root and for the third period data a natural logarithmic transformation (with zero values changed into 0.01 kg/m²) was performed, since this increases the approximation of the sample distribution towards a Gaussian population.

The data set has been analyzed for spatial patterns using variograms for each of the three periods and for the total duration. The spherical and Gaussian models showed the best fit for the sediment transport during the different periods (Table 4) and thus were used for providing the needed spatial continuity. These models were selected based on the high spatial structure of the input data, and the good fit with the sill (C+Co) and nugget (Co) points used for the kriging. The range and sill parameters explain the structure of the spatial variation and estimate the unsampled locations with the kriging method (Chappell & Agnew 2001, Chappell & Oliver 1997). The spatial interrelation of the erosion data was assessed by C/(C+CO), which ranges 0–1 (where "1" stands for a suitable spatial interrelation and "0" stand for a weak spatial interrelation and high nugget effect).

All three sediment transport periods were characterized by high $C/(C+C_O)$ values as shown in Table 4. This shows that this geostatistical approach is a suitable tool for the estimation of the erodibility of land by aeolian processes.

The highest spatial interrelationship ($C/(C+C_O)$) was found for the periods 3 (0.99) and 1 (0.97), while for the period 2, as the transitional phase between the "120 windy days" and the winter season wind regime, showed a weaker (0.81) spatial pattern of the sediment transport data. This spatial variability is also apparent by the much larger nugget value for period 2. The geostatistical parameters calculated for the whole period from August to November also showed a weaker spatial interrelation, which emphasizes the importance of shorter time slices for the analysis of spatial patterns.

The data points and the fitted models are displayed in Figure 6. This clearly shows that the sediment transport rates have changed between August and November of 2013.

The results of the variogram analysis show that the sediment transport was characterized by a high spatial dependence during the different periods. Therefore the assessment of the aeolian transport by combining the pin method with geostatistic models is acceptable in the Sistan region with its unimodal wind direction scheme during the Sadobist roozeh wind period. The high spatial interrelation detected in this study (Table 4) is an indicator for less homogeneous natural conditions with regards to vegetation cover, soil crusting and land management. Other studies found much smaller spatial dependencies in a small cultivated field (60 × 40 m) in Niger (Sterk & Stein 1997) and in three different geomorphic landscape units (valley, dune and degraded plot) in Burkina Faso (Visser et al. 2004).

The sediment transport rates recorded in the Baringak Lake showed a large range variability between the three periods (1,579–3,566 m) and the range for the total duration was even greater (4,830 m). These ranges (and their variance) are much larger than the 676 to 2,344 m ranges (high spatial interrelation ratios) detected by Chappell

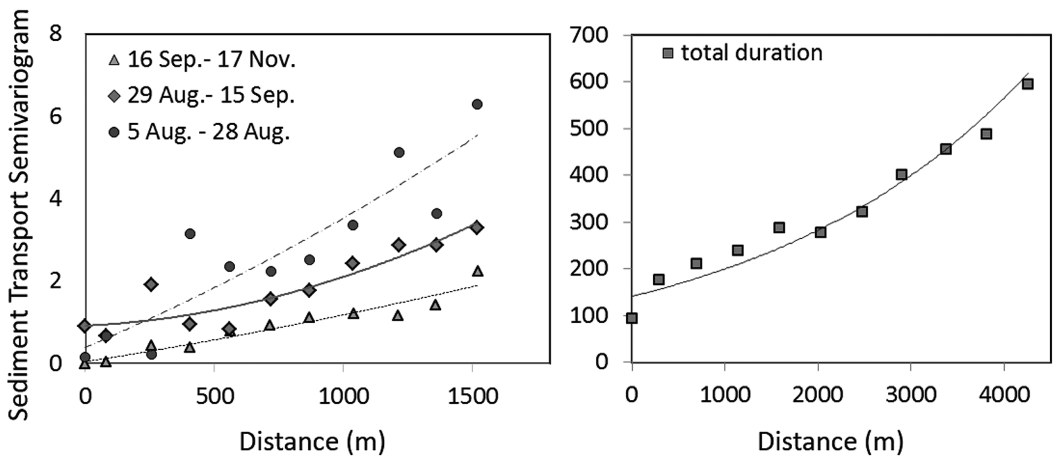

Fig. 6. Aeolian sediment transport rate variograms (point data) and fitted models (lines) for the three periods and the total duration for the Baringak Lake.

Table 5. Validation of the kriging interpolation for the sediment transport rates.

Date and event	No. of pins	Mean Absolute Error (MAE)		Root Mean Square Error (RMSE)	
		kg/m²	%	kg/m²	%
1.: 05.08.–25.08.2013	74	585.7	9.98	11.5	64.23
2.: 26.08.–15.09.2013	74	484.7	14.84	8.8	82.79
3.: 16.09.–17.11.2013	66	79.9	8.97	2.3	90.22
Total	74	703.7	1.46	12.5	40.49

et al. (2003) based on a 40 sampler campaign covering eight events in an Australian clay pan.

The results of the kriging interpolation of the sediment transport rate have been cross validated for all three periods and the total duration (Table 5). This validation focusses on the prediction issue, which evaluates the overall deviation of the predicted values from the observed values. This overall deviation is calculated by the mean absolute error (MAE) and the root-mean-square error (RMSE). The MAE indicates the accuracy of the fitted models and the resulting sediment transport maps. The MAE results show that the rate was smallest for the total study period (1.46%), while the much higher rate for the second period (14.8%) represents transition time between summer and winter wind regimes.

4.4 Mapping of the aeolian sediment transport

The final results of the geostatistical analysis are the kriging maps of the sediment transport rates for each of the three periods as well as for the whole duration of this study (Fig. 7). As seen in these maps, the largest transport rate was detected during the first period, which was heavily influenced by the "120 windy days" wind regime. During this period, the highest sediment transport occurred in the southeastern part of the study area, near the beginning of the Gorgoori and Niyatak corridors. These corridors are very active sand transport pathways from the Sistan plain into Afghanistan. During the second period, the area of the highest sediment transport activity shifted towards the south and the northwest. Towards the end of the study period the wind energy decreased and thus large areas of the lake's surface did not contribute significantly to the aeolian sediment transport. For the whole study duration from August to November two main centers of wind erosion activity were identified – one in the southeast of the Baringak lake and the other one in the northwest.

These results show the high spatial variability of the wind erosion potential and emphasize the need for a high resolution ground based research approach when spatial decisions need to be made.

5 Conclusion

The application of the pin method for measuring the sediment transport rate and the mapping of the aeolian transport rate using a geostatistics model resulted in detailed

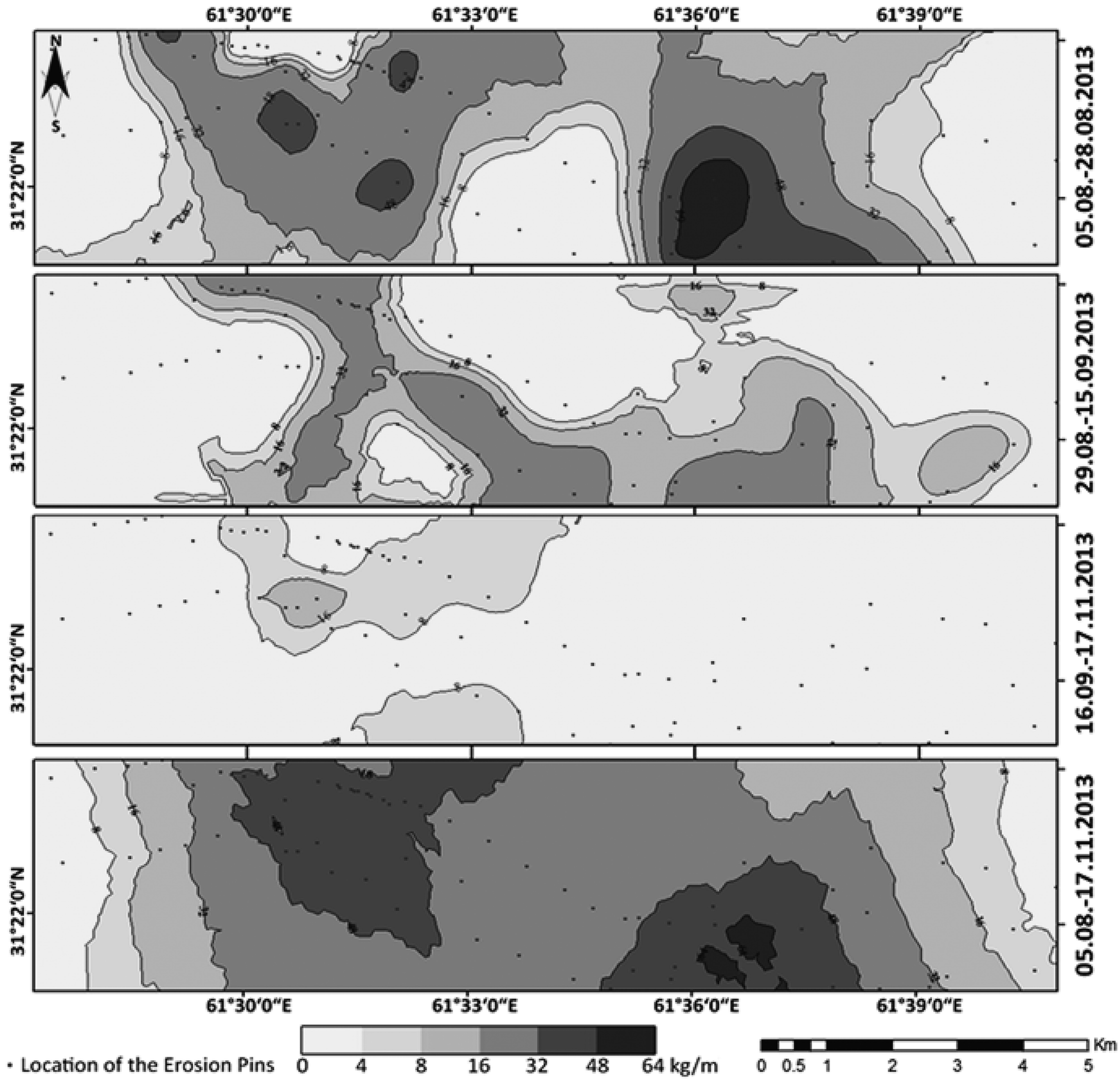

Fig. 7. Erosion pin locations and sediment transport rate (kg/m^2) in the Baringak Lake for the three periods and the total duration, estimated using ordinary kriging.

data about the temporal and spatial distribution of the wind erosion activity in the Baringak Lake. The Hamoun Baringak Lake plays a bold role for the aeolian mobilization of sediments in the Sistan region because of the hydrological droughts, frequently affecting the lake since the construction of several dams in the upper Hirmand River catchment in Afghanistan, its higher elevation (about 1 meter) than Puzak and Saberi lakes and thus shallow lake bed which is prone to falling dry early in the year, and the gradual decline of the wetland vegetation cover. The results show that the aeolian transport rate is highly variable both in time and space during the three time periods covered by this study. This study helped to identify the main sources of the aeolian sediment transport throughout the duration of measurements. Due to the wide extent of the sources of dust and sand production in Sistan, finding areas that are prone to wind erosion is of paramount importance in prioritizing stabilization. The two most active areas should now be prioritized for land management measures in order to minimize the aeolian dust and sand transport in the future. Plantation native vegetation and conservation lands from over grazing can be decrease land sensivity to wind erosion.

Furthermore the results show the great spatial and temporal variability of the sediment fluxes – even in a region characterized by a unimodal wind regime. This highlights the importance of an in depth and high resolution research setup for any future studies.

References

Ahmadi, H. (2006): Applied Geomorphology-Desert-Wind Erosion. – Tehran University, Publications, 474–475 pp.

Akhavan, R. (2010): Spatial variability and estimation of tree attributes in a plantation forest in the Caspian region of Iran using geostatistical analysis. – Caspian Journal of Environmental Sciences 8 (2): 163–172.

Alizadeh-Choobari, O., Zawar-Reza, P. & Sturman, A. (2014): The wind of 120 days and dust storm activity over the Sistan Basin. – Atmospheric Research 143: 328–341.

Belnap, J. & Gillette, D.A. (1998): Vulnerability of desert biological soil crusts to wind erosion: the influences of crust development, soil texture, and disturbance. – Journal of Arid Environments 39 (2): 133–142.

Bertrand, F. (2010): Fluvial erosion measurements of streambank using Photo-Electronic Erosion Pins (PEEP). – University of Iowa MS Thesis, accessed November 23, 2014, at http://ir.uiowa.edu/etd/642.

Burrough, P.A. & McDonald, A. (1986): Principles of geographical information systems for land resources assessment. Claredon Press, Oxford, 193 pp.

Busche, D., Grunert, J., Sarwati, R. & Pohlmann, H. (1990): Iran: Geomorphology (Eastern Part). Tübinger Atlas des Vorderen Orients TAVO, A III 3.

Casagli, N., Rinaldi, M., Gargini, A. & Curini, A. (1999): Pore water pressure and streambank stability: results from a monitoring site on the Sieve River, Italy. – Earth Surface Processes and Landforms 24 (12): 1095–1114.

Chappell, A. & Agnew, C.T. (2001): Geostatistical analysis and numerical simulation of West African Sahel rainfall. – Land Degradation, Springer 58: 19–35.

Chappell, A., McTainsh, G., Leys, J. & Strong, C. (2003a): Simulations to optimize sampling of aeolian sediment transport in space and time for mapping. – Earth Surface Processes and Landforms 28 (11): 1223–1241.

Chappell, A., McTainsh, G., Leys, J. & Strong, C. (2003b): Using geostatistics to elucidate temporal change in the spatial variation of aeolian sediment transport. – Earth Surface Processes and Landforms 28 (6): 567–585. doi: 10.1002/esp.463.

Chappell, A. & Oliver, M. (1997): Geostatistical analysis of soil redistribution in SW Niger, West Africa. – Quantitative Geology and Geostatistics 8 (2): 961–972.

Chepil, W. (1945): Dynamics of wind erosion: I. Nature of movement of soil by wind. – Soil Science 60 (4): 305–320.

Denk, W. & Müller, G. (1990): Iran and Afghanistan. – Relief, Hydrology and Sediments. Tübinger Atlas des Vorderen Orients TAVO, A I 3.

Goudie, A. & Middleton, N.J. (2006): Desert dust in the global system. – Springer Science & Business Media, 288 pp.

Groll, M., Opp, C. & Aslanov, L. (2013): Spatial and temporal distribution of the dust deposition in Central Asia – results from a long term monitoring program. – Aeolian Research 9: 49–62.

Hadley, R.F. & Lusby, G.C. (1967): Runoff and hillslope erosion resulting from a high – intensity thunderstorm near Mack, western Colorado. – Water Resources Research 3 (1): 139–143.

Haigh, M. (1977): The use of erosion pins in the study of slope evolution. – British Geomorphological Research Group Technical Bulletin 18: 31–49.

Hengl, T. (2009): A practical guide to geostatistical mapping. – University of Amsterdam, 291 pp.

Herrmann, L., Stahr, K. & Jahn, R. (1999): The importance of source region identification and their properties for soil-derived dust: the case of Harmattan dust sources for eastern West Africa. – Contributions to atmospheric physics 72 (2): 141–150.

Hooke, J. (1980): Magnitude and distribution of rates of river bank erosion. – Earth Surface processes 5 (2): 143–157.

Horn, D.P. & Lane, S.P. (2006): Measurement of high-frequency bed level changes in the swash zone using Photo-Electronic Erosion Pins (PEEPS). – Coastel Engineering Conference, World Scientific, 2591 p.

Lancaster, N. & Baas, A. (1998): Influence of vegetation cover on sand transport by wind: field studies at Owens Lake, California. – Earth Surface Processes and Landforms 23 (1): 69–82.

Lawler, D.M. (2001): The photo-electronic erosion pin (PEEP) automatic erosion monitoring system: principles and applications. – 7th Federal Interagency Sedimentation Conference on 'Sediment: Monitoring, Modeling and Managing', March 25–29, Vol. 1, P56–P59.

Li, F.R., Kang, L.F., Zhang, H., Zhao, L.Y., Shirato, Y. & Taniyama, I. (2005): Changes in intensity of wind erosion at different stages of degradation development in grasslands of Inner Mongolia, China. – Journal of Arid Environments 62 (4): 567–585.

McDermott, J.P. & Sherman, D.J. (2009): Using photo-electronic erosion pins for measuring bed elevation changes in the swash zone. – Journal of Coastal Research 25 (3): 788–792.

Middleton, N.J. (1986a): Dust storms in the Middle East. – Journal of Arid Environments, 10 (2): 83–96.

Miri, A., Moghaddamnia, A., Pahlavanravi, A. & Panjehkeh, N. (2010): Dust storm frequency after the 1999 drought in the Sistan region, Iran. – Climate Research 41 (1): 83–90.

Oldemann, L.R. (1992): Global extent of soil degradation. – ISRIC Bi-Annual Report 1991–1992, International Soil Reference and Information Centre (ISRIC), Wageningen, The Netherlands, 19–36 pp.

Oliver, M., Webster, R. & Gerrard, J. (1989): Geostatistics in physical geography. Part II: applications. – Transactions of the Institute of British Geographers 14 (3): 270–286.

Opp, C. (1998): Geographische Beiträge zur Analyse von Bodendegradationen und ihrer Diagnose in der Landschaft. – Leipziger Geowissenschaften 8, Leipzig, 187 pp.

Opp, C., Groll, M., Aslanov, I., Lotz, T., Vewreshagina, N. (2016): Aeolian dust deposition in the southern Aral Sea region (Uzbekistan): Ground-based monitoring results from the LUCA project. – Quaternary International (2016), http://dx.doi.org/10.1016/j.quaint.2015.12.103.

Peel, M.C., Finlayson, B.L. & McMahon, T.A. (2007): Updated world map of the Köppen-Geiger climate classification. –

Hydrology and earth system sciences discussions 4 (2): 439–473.
Poortinga, A., Keijsers, J., Visser, S., Riksen, M. & Baas, A. (2015): Temporal and spatial variability in event scale aeolian transport on Ameland, The Netherlands. – Geo. Res. J. 5: 23–35.
Rashki, A., Kaskaoutis, D., Goudie, A. & Kahn, R. (2013): Dryness of ephemeral lakes and consequences for dust activity: the case of the Hamoun drainage basin, southeastern Iran. – Science of the Total Environment 463: 552–564.
Ravi, S., Breshears, D.D., Huxman, T.E. & D'Odorico, P. (2010): Land degradation in drylands: Interactions among hydrologic-aeolian erosion and vegetation dynamics. – Geomorphology 116 (3): 236–245.
Reich, P., Eswaran, H. & Beinroth, F. (1999): Global dimensions of vulnerability to wind and water erosion. – In: Stott, D.E., Mohtar, R.H. & Steinhardt, G.C. (eds.): Sustaining the global farm. – Selected papers from the 10th International Soil Conservation Organization Meeting at the Purdue University and the USDAARS National Soil Erosion Research Laboratory, West Lafayette, USA, 24–29 May, 838–846.
Robinson, T. & Metternicht, G. (2006): Testing the performance of spatial interpolation techniques for mapping soil properties. – Computers and electronics in agriculture 50 (2): 97–108.
Sharifikia, M. (2013): Environmental challenges and drought hazard assessment of Hamoun Desert Lake in Sistan region, Iran, based on the time series of satellite imagery. – Natural Hazards 65 (1): 201–217.
Shi, W., Fisher, P. & Goodchild, M.F. (2003): Spatial data quality. – CRC Press, Boca Raton, 340 pp.
Sterk, G. & Stein, A. (1997): Mapping wind-blown mass transport by modeling variability in space and time. – Soil Science Society of America Journal 61 (1): 232–239.
Takei, A., Kobashi, S. & Fukushima, Y. (1981): Erosion and sediment transport measurement in a weathered granite mountain area. – Publ. IAHS 133: 493–501.
Uzun, O., Kaplan, S.., Basaran, M., Deviren Saygın, S., Youssef, F., Nouri, A., Ozcan, A.U. & Erpul, G. (2017): Spatial distribution of wind-driven sediment transport rate in a fallow plot in Central Anatolia, Turkey. – Arid Land Research and Management 31 (2): 125–139.
Vekerdy, Z., Dost, R., Reinink, G. & Partow, H. (2006): History of environmental change in the Sistan Basin based on satellite image analysis: 1976–2005. Report, United Nations Environmental Programme (UNEP) and ITC, 60 pp. http://postconflict.unep.ch/publications/sistan.pdf
Visser, S.M., Sterk, G. & Snepvangers, J.J. (2004): Spatial variation in wind-blown sediment transport in geomorphic units in northern Burkina Faso using geostatistical mapping. – Geoderma 120 (1): 95–107.
Webster, R. & Oliver, M.A. (2001): Geostatistics for Environmental Scientists. Statistics in Practice. – Wiley, Chichester, 265 pp.
Weinan, C. & Fryrear, D.W. (1996): Grain-size distributions of wind-eroded material above a flat bare soil. – Physical Geography 17 (6): 554–584.
Whitney, J.W. (2006): Geology, water, and wind in the lower Helmand Basin, Southern Afghanistan. – US Geological Survey Scientific Investigation Report: 5182, 40 pp.
Wolfe, S.A. & Nickling, W.G. (1993): The protective role of sparse vegetation in wind erosion. – Progress in Physical Geography 17: 50–50.
Wolman, M.G. (1959): Factors influencing erosion of a cohesive river bank. – American Journal of Science 257 (3): 204–216.

Manuscript received: January 23, 2017
Revisions required: November 6, 2017
Revised version received: December 19, 2017
Accepted: December 21, 2017